Wenle Weng and Andre N. Luiten
Mode-interactions and polarization conversion in a crystalline microresonator
Optics Letters, 2015; 40(23):5431-5434

Online abstract http://dx.doi.org/10.1364/OL.40.005431

Mode-interactions and polarization conversion in a crystalline microresonator

WENLE WENG[1,2,*] AND ANDRE N. LUITEN[1,2]

[1] Institute for Photonics and Advanced Sensing and School of Physical Sciences, University of Adelaide, SA 5005, Australia
[2] School of Physics, University of Western Australia, WA 6009, Australia
[*] Corresponding author: wenle.weng@adelaide.edu.au

Compiled October 23, 2015

We observe couplings between orthogonally-polarized modes in a birefringent whispering-gallery-mode resonator. The modes show strong interactions leading to polarization conversion and avoided mode crossings. We show that a phenomenological model, based on coupled-mode theory, is in good agreement with the experiments. The device provides an excellent laboratory to perform controllable and tunable mode interactions.

OCIS codes: *(140.4780) Optical resonators; (140.6810) Thermal effects; (130.5440) Polarization-selective devices; (160.1190) Anisotropic optical materials.*

http://dx.doi.org/10.1364/ao.XX.XXXXXX

There has been much interest in observing coupling between different modes in whispering-gallery-mode resonators (WGMR). These couplings alter the mode spectra, modify the field dynamics, and can be used to beneficial effect in sensing and optomechanical experiments [1–4]. While most effort has been aimed at understanding scattering-induced coupling between forward- and backward-propagating modes, there has been some effort to observe coupling between orthogonally-polarized modes [5]. This type of coupling has also been studied in fiber and waveguide resonators, where the effect influences the dispersive properties and has prospective applications in polarization conversion and nonlinear frequency generation [6, 7].

The production of a desired level of mode coupling requires precise control of the position and strength of an exterior scatter [1, 8], or intimate control of the resonator geometry or material parameters [9, 10]. Ioannidis *et al*. [11] circumvented these challenging requirements by temperature tuning a fiber ring resonator and were able to explain their observations using a matrix method.

In this work, we extend this approach to show highly controllable polarization conversion in a birefringent WGMR by adjusting the relative detuning of two modes through a differential thermooptic effect. We then exploit the extremely low losses of the resonator to show much stronger mode interactions: we demonstrate mode interactions that possess a clear avoided mode-crossing, emphasising that the mode coupling strength is substantially higher than any dissipative processes.

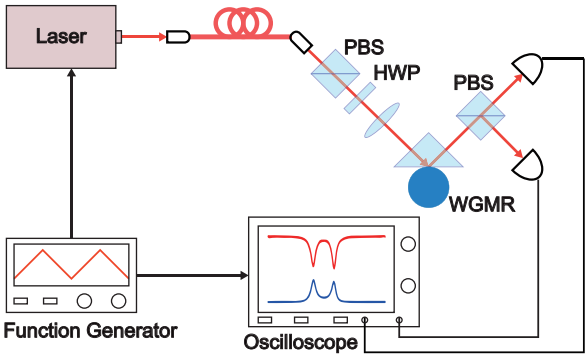

Fig. 1. The resonator was driven by light with carefully tailored polarization. The polarization state of the transmitted light is polarization analyzed and then falls on two photodiodes. HWP: half-wave plate; PBS: polarizing beam splitter.

The experimental setup is presented in Fig. 1. The output of a 1064-nm Nd:YAG laser is coupled into a MgF_2 WGMR using a coupling prism. The resonator is a disk with a radius of 5 mm and a thickness of 1 mm with its output edge polished to a radius of curvature of 1 mm. A thermistor-heater pair is attached to the center of the resonator to control the temperature. The laser power is kept low to eliminate observable thermal nonlinearity [12, 13]. The resonator's optical axis has been carefully aligned with the geometric axis to within 5° (Z-cut).

The resonator is mounted in a hermetic shielded environment and the laser light is transfer to the prism coupler with polarization-maintaining fiber. The polarization of the light is carefully set using a polarizer and a half-wave plate. The transmitted beam's polarization is analyzed using a polarization beam splitter which then feeds two photodetectors. When no light is coupled to the resonator, either because of a large frequency detuning between the mode and the laser, or because of a large spacing between the prism and the resonator, then we see less than 0.1% cross-coupling between either of the input polarization states and the opposite output polarization state. This residual cross-coupling is associated with the imperfect extinction ratio of the output and input polarization beam splitters.

Fig. 2 shows the measured and calculated transmission spec-

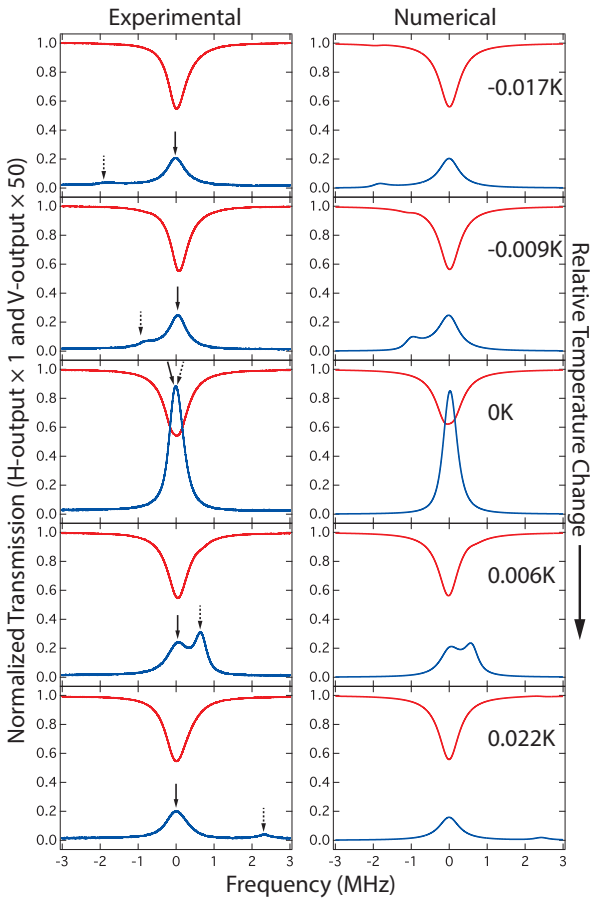

Fig. 2. The observed (left-hand panels) and calculated (right-hand panels) spectra for the horizontal (red) and vertical polarization (blue) outputs. The different vertical panels show the output at different relative resonator temperatures. The solid arrows point to the TE mode, while the dashed arrows indicate the positions of TM mode. The amplitude of the transmission of the vertical polarization has been multiplied by a factor of 50 to increase clarity. The TM mode is only just visible in the vertical polarization when the detuning is large because of its low amplitude and the limited signal-to-noise ratio of the spectra.

tra as the resonator temperature is varied. For this first experiment the input beam is adjusted to be horizontally polarized, which can couple to the fundamental TE modes of the resonator (see dip in center of the frequency scans shown on Fig. 2). The coupling into the vertical output polarization is relatively weak and we have thus multiplied the measured transmission by 50 to improve clarity on the figure. We re-tune the laser for each of the temperatures displayed on Fig. 2 so as to keep the TE mode centered in the scan.

We note that a weak polarization conversion effect is observed when the laser is in resonance with the TE mode - (see the top left hand panel of Fig. 2 as an example). The fractional conversion is only 1% and arises from a mismatch of the eigenpolarizations of the resonator modes and the linear polarization of the free space modes. It is not possible to eliminate this effect by rotating the input linear polarization. This observation shows that the resonator eigenmodes contain some ellipticity or spatially non-uniform polarization - this is to be expected because of resonator curvature, residual stress and misalignment of the geometric and optical axes [14, 15].

As we travel downwards on the panels of Fig. 2 we observe the effects of a resonator temperature change on the spectra. We see a second mode that is of predominantly TM character (shown by the fact it can be principally observed in the TM output channel when it is detuned from the TE mode) tune through the main mode. A relative tuning of the two modes is possible because of the difference in thermooptic coefficients for the TE and TM modes in birefringent MgF_2. As the smaller mode tunes across the stronger TE mode we see a strong increase in the strength of the polarization conversion. A highest conversion efficiency of $\sim 4\%$ was observed (see the middle left hand panel of Fig. 2) when the the frequency of the two modes is tuned into coincidence.

We deduce that this polarization conversion is caused by mode interaction between the orthogonally polarized modes. The cross-polarization coupling can arise from sidewall scattering or through small spatial variations in the birefringence in the resonator [5, 11, 16]. We use coupled-mode theory [17] to calculate the amplitude of two eigenmodes, $\tilde{a}$, $\tilde{b}$ in the resonator:

$$\frac{d\tilde{a}}{dt} = -(i\omega_a + \gamma_a + \Gamma_a)\tilde{a} - ig\tilde{b} - \kappa_a\tilde{a}_{in} \quad \textbf{(1)}$$

$$\frac{d\tilde{b}}{dt} = -(i\omega_b + \gamma_b + \Gamma_b)\tilde{b} - ig\tilde{a} - \kappa_b\tilde{b}_{in} \quad \textbf{(2)}$$

where ω_a and ω_b are the angular mode frequency, and γ_a, γ_b, Γ_a and Γ_b are the intrinsic loss rates and prism coupling loss rates of the two modes respectively. g denotes the coupling strength between the two modes. The mode frequency difference can be related to changes in the temperature through $\omega_b - \omega_a = \alpha\Delta T$, where ΔT is the resonator temperature difference from some fixed value, and α is determined by the difference in the TE and TM thermooptic coefficients. The value of α can be estimated as $-110 \pm 20\,\mathrm{MHz/K}$ from the known thermooptic coefficients of $dn_o/dT = 0.89 \times 10^{-6}/\mathrm{K}$ and $dn_e/dT = 0.34 \times 10^{-6}/\mathrm{K}$ [18]. The error bound was estimated from the inconsistency between the theory and experimental data at the nearest wavelength data provided in [18] and serves only as lower bound.

The coefficients κ_a, κ_b can be related to the coupling loss rates as: $\kappa_{a,b} = \sqrt{2\Gamma_{a,b}}$ respectively. However, the effects of mode-matching at coupling-in process can substantially reduce the observed κ. We observed that the in-coupling to the TM mode shown on Fig. 2 was exceedingly low for any adjustment of input angle or beam size – this provides strong evidence that the TM mode that is excited through the modal cross-coupling has a high angular and/or radial mode number. The low input coupling was expressed in our model by setting $\kappa_b \sim 0$.

We allow for polarization mismatch between the input fields $\tilde{a}_{in}, \tilde{b}_{in}$ and the resonator eigenmodes, $\tilde{a}, \tilde{b}$ by including a Jones matrix, $M = \begin{bmatrix} \cos(\theta) & \sin(\theta) \\ -\exp(-i\eta)\sin(\theta) & \exp(-i\eta)\cos(\theta) \end{bmatrix}$, that allows for arbitrary polarization rotation, θ, and phase retardation, η i.e. $\begin{bmatrix} \tilde{a}_{in} \\ \tilde{b}_{in} \end{bmatrix} = M \begin{bmatrix} \tilde{E}_h \\ \tilde{E}_v \end{bmatrix}$, where $\tilde{E}_h$ and $\tilde{E}_v$ denote the horizontally and vertically polarized input fields respectively. The values of θ and η are determined as part of the fitting procedure. At the resonator output, the transmitted fields of TE and TM modes are a sum of the input and out-coupled fields $E_o = \begin{bmatrix} \tilde{a}_{in} + \kappa_a\tilde{a} \\ \tilde{b}_{in} + \kappa_b\tilde{b} \end{bmatrix}$. The

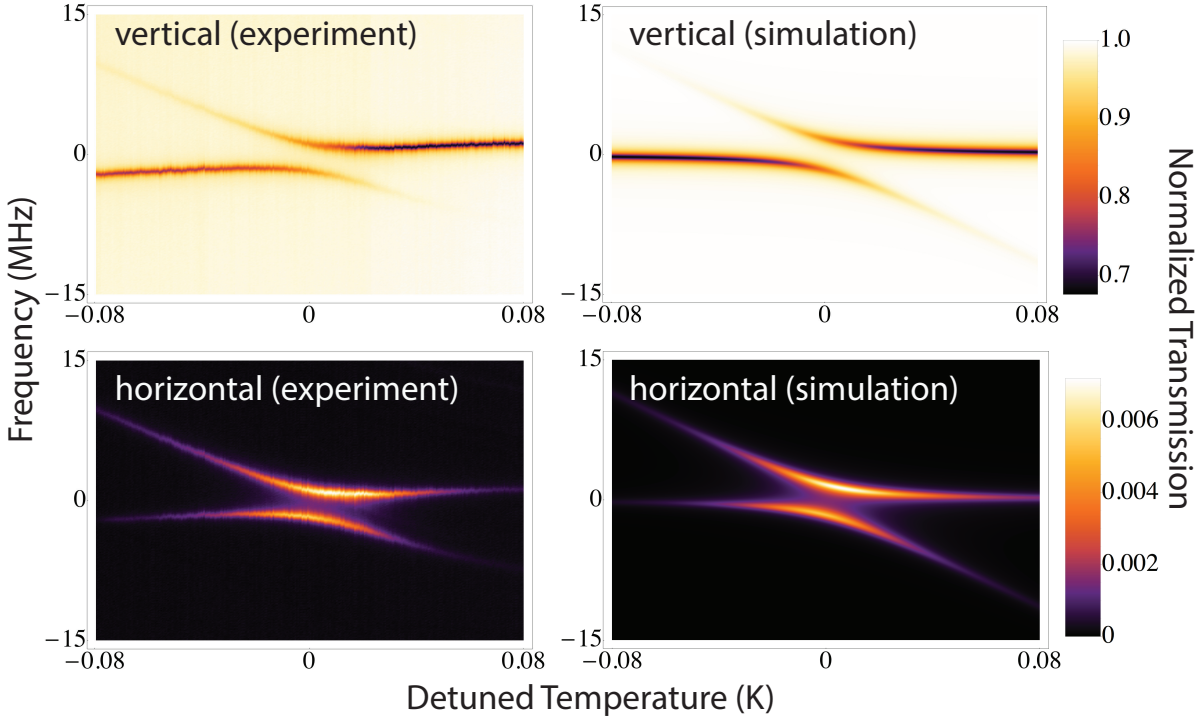

Fig. 3. Experimental and simulated transmission spectra as observed in two orthogonal polarizations with vertical polarization excitation. The upper (lower) panels show the vertical (horizontal) polarization respectively. Not only is polarization conversion clearly seen but also an avoided mode crossing. The experimental data shows a slight tilt when compared to theory because the anchor mode (not shown in the figures) and the TM mode do not have exactly the same temperature sensitivity.

fields registered on the two photodetectors have been projected onto the free-space modes, E_H and E_V, as $\begin{bmatrix} E_H \\ E_V \end{bmatrix} = M^{-1}E_o$.

The solutions of the normalized transmissions detected by the two photodetectors are shown on the right-hand panels of Fig. 2, which agree very well with the experimental observations using $\gamma_a = 2.8 \times 10^5 \times 2\pi$, $\gamma_b = 1.8 \times 10^5 \times 2\pi$, $\Gamma_a = 4.3 \times 10^4 \times 2\pi$, $\Gamma_b = 3.4 \times 10^4 \times 2\pi$, $g = 9 \times 10^4 \times 2\pi$, $\theta = 0.23$ and $\eta = 1.95$.

The model was tested with greater stringency by exciting two modes that had a much stronger coupling than those described earlier and by also using a frequency comb to measure the absolute mode frequency of both modes. For this second experiment we have chosen to predominately excite TM modes using a vertically polarized input beam. This was to show that the same types of mode interaction were observable irrespective of the polarization of the exciting mode: similar behavior could be observed with TE excitation. Due to the complexity of the mode structure and the high mode density in millimeter-scale resonators, we did not identify the mode numbers of the modes, although, the imaging method in [19] could be utilized. We used a third mode that was a few tens of MHz away from the targeted interacting modes as an *in situ* temperature probe. The mode frequency was measured using a stabilized frequency comb with a fractional frequency accuracy better than 10^{-12}. We calculated the mode-frequency temperature sensitivity of the probe mode of $df/dT \approx 2.8\,\mathrm{GHz/K}$ [18] and then used this coefficient to convert the measured frequency to a temperature change, ΔT.

Fig. 3 shows both the observed and simulated spectral maps as recorded by photodetectors recording the intensity of transmitted light in the two orthogonal output polarizations. Vertical (horizontal) output polarization is shown in the upper (lower) panels. The color of the map is proportional to the transmitted intensity at various frequencies while the horizontal axis records the relative temperature of the resonator. The right hand side shows the experimentally measured results while the left hand side shows a simulation using the values $\gamma_a = 3 \times 10^5 \times 2\pi$, $\gamma_b = 4.7 \times 10^5 \times 2\pi$, $\Gamma_a = \Gamma_b = 3.5 \times 10^4 \times 2\pi$, $g = 1.68 \times 10^6 \times 2\pi$, $\theta = 0.093$ and $\eta = 2.39$. We can see that there is excellent agreement between the model and the measured results. We clearly see an avoided crossing with a minimum frequency spacing of ~ 4 bandwidths showing the strength of the interaction between the two modes. We see a polarization conversion of nearly 5% at this point. Through these absolute frequency measurement we can calculate an accurate value for α of $-140\,\mathrm{MHz/K}$. This is on the outside bound of the value, $-110 \pm 20\,\mathrm{MHz/K}$, provided by [18]. The extracted value for g corresponds to a mode splitting of $\sim$3.3 MHz when $\Delta T = 0\,\mathrm{K}$. The ratio of the mode coupling to dissipation, $g/(\Gamma_{a,b} + \gamma_{a,b})$, is around 5 in contrast to the earlier example on Fig. 2 where it was 0.2 - this explains why one only observes polarization conversion in the earlier experiment rather than mode-splitting that is reported here.

We repeated these measurements with a large number of mode pairings, and noted that the mode interaction was much stronger when at least one mode had high angular mode number. One possible reason would be that modes with high angular mode number have larger sidewall angles and hence higher scattering [6, 20]. Further study is demanded to fully explain the detailed mechanism that produces the dependence of the mode interaction strength on the mode type.

In Fig. 4 we plot the observed and simulated frequency split-

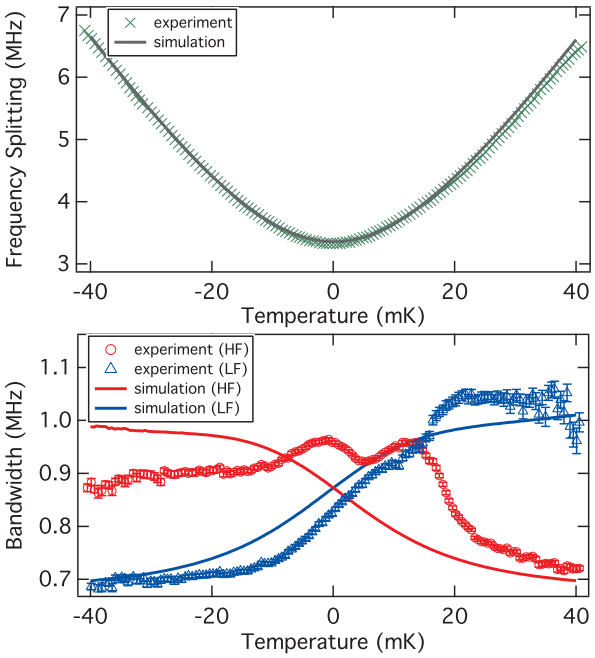

Fig. 4. (upper panel) Frequency splitting of the mode spectra excited with a vertically-polarized beam. (lower panel) Bandwidth exchange of the lower frequency mode (LF) and higher frequency mode (HF) of the horizontal spectra as a function of resonator temperature.

ting between the two modes for the same data as shown on the horizontal spectra in Fig. 3. We see excellent agreement of the frequency evolution during the mode interaction. On the lower panel of Fig. 4 we examine the mode bandwidth variation and we see only qualitative agreement. In a two-mode interaction one expects the product of the Q-factors of the two modes to be approximately constant as a function of mode detuning – the data shown on Fig. 4 clearly indicates that our experiment does not follow this expectation. In large resonators, with their associated high mode densities, there are many additional modes that provide a means for additional couplings between the observed modes. The modes can be only poorly coupled to the external environment and hence are not easily observed (similar to the reservoir modes described in [1, 8]). If we extend Eqs. 1 and 2 to allow for additional coupling paths between modes via these unobserved modes then we can reproduce the behavior observed on Fig. 4; although, this comes necessarily at the expense of an additional set of parameters that cannot be independently determined. In the circumstances in which we do not allow for these additional couplings we would only expect qualitative agreement which is indeed what is seen on the lower panel of Fig. 4.

In conclusion, we have demonstrated polarization conversion and avoided crossing in a birefringent WGMR that can be controlled through resonator temperature. A highest polarization conversion efficiency of nearly 5% was observed. Our phenomenological model showed that these effects can be explained through the strong coupling between orthogonally polarized modes. We presented two detailed examples: one where the normalized mode coupling strength was less than one, and a second where it greatly exceeded one. The thermooptic coefficients of the birefringent material give excellent control of the coupling strength as well as the ability to follow the process in great detail. This mechanism can provide an extra method for dispersion engineering for Kerr comb generation and has the potential to increase the versatility of WGMR for signal processing applications. On the other hand, the polarization coupling effect reported in this work can have a disruptive effect on dual-mode temperature measurements using WGMRs [21] and also interrupt the formation of temporal solitons under otherwise appropriate conditions [22, 23]. It is thus vital to have a good understanding of the effect to avoid these deleterious effects.

FUNDING INFORMATION

Australian Research Council (ARC) (DP0877938, FT0991631, LE110100054, LE100100009); South Australian Government Premier's Science and Research Fund.

REFERENCES

1. A. Mazzei, S. Götzinger, L. d. S. Menezes, G. Zumofen, O. Benson, and V. Sandoghdar, Physical review letters **99**, 173603 (2007).
2. J. Zhu, S. K. Ozdemir, Y.-F. Xiao, L. Li, L. He, D.-R. Chen, and L. Yang, Nat. Photonics **4**, 46 (2009).
3. J. Wiersig, Phys. Rev. Lett. **112**, 203901 (2014).
4. M. Aspelmeyer, T. J. Kippenberg, and F. Marquardt, Reviews of Modern Physics **86**, 1391 (2014).
5. A. Melloni, F. Morichetti, and M. Martinelli, Optics letters **29**, 2785 (2004).
6. S. Ramelow, A. Farsi, S. Clemmen, J. S. Levy, A. R. Johnson, Y. Okawachi, M. R. Lamont, M. Lipson, and A. L. Gaeta, Optics letters **39**, 5134 (2014).
7. Y. Liu, Y. Xuan, X. Xue, P.-H. Wang, S. Chen, A. J. Metcalf, J. Wang, D. E. Leaird, M. Qi, and A. M. Weiner, Optica **1**, 137 (2014).
8. J. Zhu, Şahin Kaya Özdemir, L. He, and L. Yang, Opt. Express **18**, 23535 (2010).
9. S. Wang, K. Broderick, H. Smith, and Y. Yi, Applied Physics Letters **97**, 051102 (2010).
10. I. S. Grudinin and N. Yu, Optica **2**, 221 (2015).
11. Z. K. Ioannidis, R. Kadiwar, and I. Giles, Optics letters **14**, 520 (1989).
12. T. Carmon, L. Yang, and K. Vahala, Optics Express **12**, 4742 (2004).
13. W. Weng, J. D. Anstie, P. Abbott, B. Fan, T. Stace, and A. N. Luiten, Physical Review A **91**, 063801 (2015).
14. F. Sedlmeir, M. Hauer, J. U. Fürst, G. Leuchs, and H. G. Schwefel, Optics express **21**, 23942 (2013).
15. Z. Zhu and T. G. Brown, Optics letters **28**, 2306 (2003).
16. B. E. Little and S. T. Chu, IEEE Photonics Technology Letters **12**, 401 (2000).
17. H. A. Haus, *Waves and fields in optoelectronics*, Vol. 464 (Prentice-Hall Englewood Cliffs, NJ, 1984).
18. G. Ghosh, *Handbook of Optical Constants of Solids: Handbook of Thermo-Optic Coefficients of Optical Materials with Applications* (Academic Press, 1998).
19. G. Schunk, J. U. Fürst, M. Förtsch, D. V. Strekalov, U. Vogl, F. Sedlmeir, H. G. Schwefel, G. Leuchs, and C. Marquardt, Optics Express **22**, 30795 (2014).
20. F. Morichetti, A. Canciamilla, C. Ferrari, M. Torregiani, A. Melloni, and M. Martinelli, Physical review letters **104**, 033902 (2010).
21. D. V. Strekalov, R. J. Thompson, L. M. Baumgartel, I. S. Grudinin, and N. Yu, Opt. Express **19**, 14495 (2011).
22. T. Herr, V. Brasch, J. Jost, C. Wang, N. Kondratiev, M. Gorodetsky, and T. Kippenberg, Nature Photonics **8**, 145 (2014).
23. T. Herr, V. Brasch, J. Jost, I. Mirgorodskiy, G. Lihachev, M. Gorodetsky, and T. Kippenberg, Physical review letters **113**, 123901 (2014).

REFERENCES

1. A. Mazzei, S. Götzinger, L. d. S. Menezes, G. Zumofen, O. Benson, and V. Sandoghdar, "Controlled coupling of counterpropagating whispering-gallery modes by a single rayleigh scatterer: a classical problem in a quantum optical light," Physical review letters **99**, 173603 (2007).
2. J. Zhu, S. K. Ozdemir, Y.-F. Xiao, L. Li, L. He, D.-R. Chen, and L. Yang, "On-chip single nanoparticle detection and sizing by mode splitting in an ultrahigh-q microresonator," Nat. Photonics **4**, 46–49 (2009).
3. J. Wiersig, "Enhancing the sensitivity of frequency and energy splitting detection by using exceptional points: Application to microcavity sensors for single-particle detection," Phys. Rev. Lett. **112**, 203901 (2014).
4. M. Aspelmeyer, T. J. Kippenberg, and F. Marquardt, "Cavity optomechanics," Reviews of Modern Physics **86**, 1391 (2014).
5. A. Melloni, F. Morichetti, and M. Martinelli, "Polarization conversion in ring resonator phase shifters," Optics letters **29**, 2785–2787 (2004).
6. S. Ramelow, A. Farsi, S. Clemmen, J. S. Levy, A. R. Johnson, Y. Okawachi, M. R. Lamont, M. Lipson, and A. L. Gaeta, "Strong polarization mode coupling in microresonators," Optics letters **39**, 5134–5137 (2014).
7. Y. Liu, Y. Xuan, X. Xue, P.-H. Wang, S. Chen, A. J. Metcalf, J. Wang, D. E. Leaird, M. Qi, and A. M. Weiner, "Investigation of mode coupling in normal-dispersion silicon nitride microresonators for kerr frequency comb generation," Optica **1**, 137–144 (2014).
8. J. Zhu, Şahin Kaya Özdemir, L. He, and L. Yang, "Controlled manipulation of mode splitting in an optical microcavity by tworayleigh scatterers," Opt. Express **18**, 23535–23543 (2010).
9. S. Wang, K. Broderick, H. Smith, and Y. Yi, "Strong coupling between on chip notched ring resonator and nanoparticle," Applied Physics Letters **97**, 051102 (2010).
10. I. S. Grudinin and N. Yu, "Dispersion engineering of crystalline resonators via microstructuring," Optica **2**, 221–224 (2015).
11. Z. K. Ioannidis, R. Kadiwar, and I. Giles, "Polarization mode coupling in highly birefringent optical-fiber ring resonators," Optics letters **14**, 520–522 (1989).
12. T. Carmon, L. Yang, and K. Vahala, "Dynamical thermal behavior and thermal self-stability of microcavities," Optics Express **12**, 4742–4750 (2004).
13. W. Weng, J. D. Anstie, P. Abbott, B. Fan, T. Stace, and A. N. Luiten, "Stabilization of a dynamically unstable opto-thermo-mechanical oscillator," Physical Review A **91**, 063801 (2015).
14. F. Sedlmeir, M. Hauer, J. U. Fürst, G. Leuchs, and H. G. Schwefel, "Experimental characterization of an uniaxial angle cut whispering gallery mode resonator," Optics express **21**, 23942–23949 (2013).
15. Z. Zhu and T. G. Brown, "Stress-induced birefringence in microstructured optical fibers," Optics letters **28**, 2306–2308 (2003).
16. B. E. Little and S. T. Chu, "Theory of polarization rotation and conversion in vertically coupled microresonators," IEEE Photonics Technology Letters **12**, 401–403 (2000).
17. H. A. Haus, *Waves and fields in optoelectronics*, vol. 464 (Prentice-Hall Englewood Cliffs, NJ, 1984).
18. G. Ghosh, *Handbook of Optical Constants of Solids: Handbook of Thermo-Optic Coefficients of Optical Materials with Applications* (Academic Press, 1998).
19. G. Schunk, J. U. Fürst, M. Förtsch, D. V. Strekalov, U. Vogl, F. Sedlmeir, H. G. Schwefel, G. Leuchs, and C. Marquardt, "Identifying modes of large whispering-gallery mode resonators from the spectrum and emission pattern," Optics Express **22**, 30795–30806 (2014).
20. F. Morichetti, A. Canciamilla, C. Ferrari, M. Torregiani, A. Melloni, and M. Martinelli, "Roughness induced backscattering in optical silicon waveguides," Physical review letters **104**, 033902 (2010).
21. D. V. Strekalov, R. J. Thompson, L. M. Baumgartel, I. S. Grudinin, and N. Yu, "Temperature measurement and stabilization in a birefringent whispering gallery mode resonator," Opt. Express **19**, 14495–14501 (2011).
22. T. Herr, V. Brasch, J. Jost, C. Wang, N. Kondratiev, M. Gorodetsky, and T. Kippenberg, "Temporal solitons in optical microresonators," Nature Photonics **8**, 145–152 (2014).
23. T. Herr, V. Brasch, J. Jost, I. Mirgorodskiy, G. Lihachev, M. Gorodetsky, and T. Kippenberg, "Mode spectrum and temporal soliton formation in optical microresonators," Physical review letters **113**, 123901 (2014).